I dedicate this thesis to my beloved

Maa & Papa

Declaration

I hereby declare that the thesis entitled "Development of Two-Dimensional Material and Transition Metal Oxide based nanocomposites for Direct Methanol Fuel Cell Anode Catalyst and Supercapacitor Electrode", being submitted to the School of Sciences, Tezpur University in partial fulfillment of the requirements for the award of the Doctor of Philosophy in Physics, is a record of original research work carried out by me. Any text, figures, theories, results or designs that are not of my own devising are appropriately referenced in order to give due credit to the original author(s). All the sources of assistance have been assigned due acknowledgement. I also declare that neither this work as a whole nor a part of it has been submitted to any other university or institute for any degree, diploma, associateship, fellowship or any

other similar title or recognition.



Date: 07/11/2024

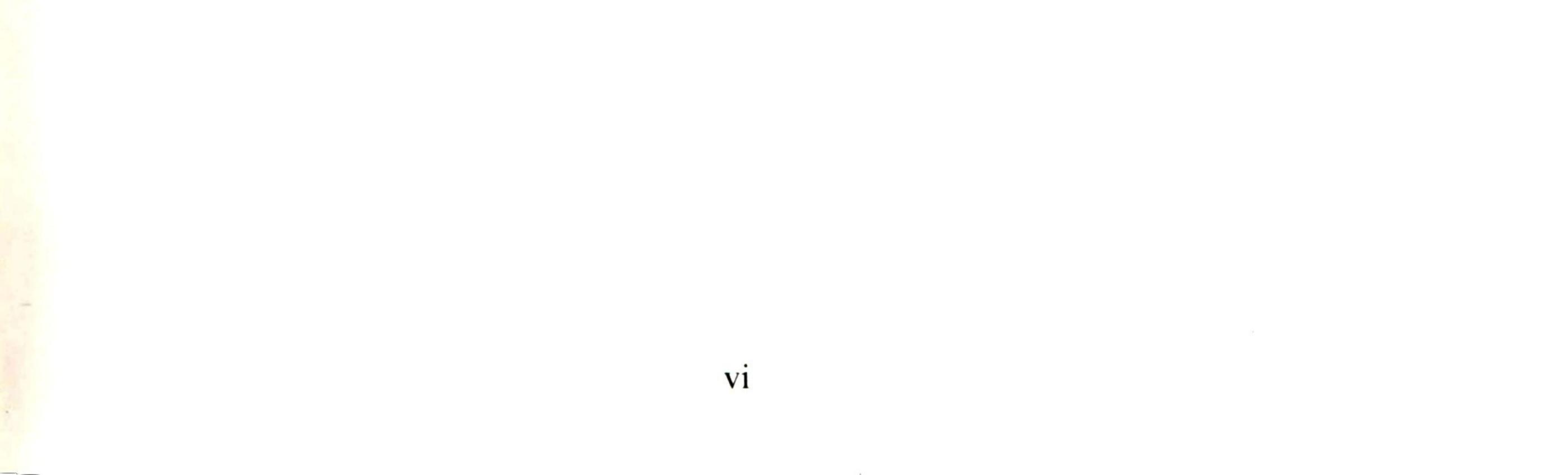
Place: Tezpur

Kashmiri Barnah

(Kashmiri Baruah)

Enrollment No:PHP18112

Registration Number: TZ132582 of 2013





Tezpur University

(A Central University established by an act of Parliament)

Department Of Physics

Tezpur – 784028, ASSAM, INDIA

Prof. Pritam Deb Professor **Department of Physics Tezpur University, Tezpur**

Ph. 03712-275560 (O) Fax: +91-3712-267005/6 Email: pdeb@tezu.ernet.in

CERTIFICATE OF THE PRINCIPAL SUPERVISOR

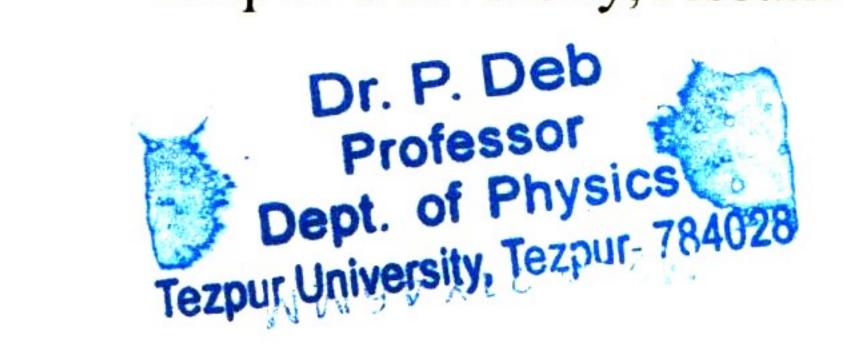
This is to certify that the thesis entitled "Development of Two-Dimensional Material and Transition Metal Oxide based nanocomposites for Direct Methanol Fuel Cell Anode Catalyst and Supercapacitor Electrode" submitted to the School of Sciences, Tezpur University in requirement of partial fulfilment for the award of the Doctor of Philosophy in Physics, is a record of original research work carried out by Ms. Kashmiri Baruah under my supervision and guidance.

All help received by her from various sources have been duly acknowledged.

No part of the thesis has been submitted elsewhere for award of any other degree.

Ant and Asle.

(Prof. Pritam Deb) Professor **Department of Physics** Tezpur University, Assam



Date: 04/11/2024. Place: Tezpur University, Assam

vii



Tezpur University (A Central University established by an act of Parliament) **Department Of Physics** Tezpur – 784028, ASSAM, INDIA

CERTIFICATE OF THE EXTERNAL EXAMINER AND ODEC

This is to certify that the thesis entitled " Development of Two-Dimensional Material and Transition Metal Oxide based nanocomposites for Direct Methanol Fuel Cell Anode Catalyst and Supercapacitor Electrode" submittedby Ms. Kashmiri Baruah to Tezpur University in the Department of Physics under the School of Sciences in partial fulfilment for the award of the

degree of Doctor of Philosophy in Physics, has been examined by us and found to be satisfactory.

The committee recommends for the award of the degree of Doctor of Philosophy.

Signatures:

Pritau Xell. Supervisor Dr. P. Deb M Professor Dept. of Physics Tezpur University, Tezpur. 784028 Date: 21/11/2024.

A. Basu Mallak

External examiner



Date: 21/11/2024 Dr. Amitava Basu Mallick Professor Metallurgy and Materials Engineering Indian Institute of Engineering Science and Technology, Shibpur Howrah - 711 103

ACKNOWLEDGEMENT

Here, I take this as my opportunity to offer my heartfelt gratitude to all those whose direct or indirect support have lifted and helped me in continuing my PhD and concluding my thesis successfully.

To start with, it gives me immense happiness to express my heartfelt gratitude and appreciation to my respected supervisor, Late Prof. Ashok Kumar for believing in me and enrolling me under his guidance. I was fortunate enough to receive his guidance, unwavering support, kindness, have fruitful scientific discussions with him and learn a lot from his vast sea of knowledge.

It gives me profound pleasure to express my sincere gratitude and appreciation to my respected supervisor, Prof. Pritam Deb for enrolling me under his guidance after the demise of Late. Prof. Ashok Kumar. His relentless support and motivation have helped me in continuing my PhD with the same enthusiasm I started my journey with. His dynamic supervision, insightful discussions and positive comments have encouraged me in carrying out my research work and improving my overall scholarly approach.

I would like to express my sincere gratitude to my doctoral committee members, Prof. Dambarudhar Mohanta and Dr. Shyamal Kumar Das of Department of Physics, Tezpur University, Assam, for their valuable suggestions, discussions, and motivation during my entire PhD tenure.

I would like to offer my genuine gratitude to the former Vice-chancellor, Prof. M. K. Chaudhuri, Prof. V.K. Jain and present Vice-chancellor Prof. S. N. Singh of Tezpur University for providing all the necessary facilities required for accomplishing PhD degree.

I express my sincere thanks to former Head, Department of Physics, Prof. Nilakshi Das, Prof. M.K. Das, Prof. Nidhi Bhattacharya; and present Head, Department of Physics, Prof. Pabitra Nath for providing the necessary facilities for research and for their encouragement. I would like to offer my gratefulness to all the faculties of Department of Physics for their encouragement throughout my PhD tenure. A special thanks to Dr. Rupjyoti Gogoi for her amicable attitude and encouragement.

I would like to offer my heartfelt gratitude to Dr. B. K. Kakati, Department of Energy for his fruitful discussions, suggestions and encouragement during my PhD tenure. I offer my heartfelt thanks to Prof. Ramesh T. Subramaniam, Department of Physics, University of Malaya and Prof. Ramesh Kasi, Department of Physics, University of Malaya for their scientific discussions and suggestions.

I am deeply grateful to Tezpur University for providing me the opportunity to pursue my PhD in the Department of Physics. The university has provided all the required laboratory facilities and the Sophisticated Analytical Instrumentation Centre (SAIC) for performing the experiments. The good hostel facilities and the excellent natural beauty of Tezpur University create a suitable healing environment which is much required for a research scholar. I shall forever remain grateful to Tezpur University for giving me such a wonderful stay and leaving me with bundles of experiences and memories.

I would like to thank University Grants Commission, New Delhi for providing me the financial support, UGC-NFOBC fellowship to carry out my research work.

I would like to acknowledge Mr. J. P. Nongkynrih of Sophisticated Analytical Instrumentation Facility (SAIF), NEHU, Shillong and Dr. Ratan Boruah, SAIC, Tezpur University for helping me with TEM measurements. I thank Dr. Manash R. Das and Rupjyoti Dutta of CSIR-NEIST, Jorhat for helping me with XPS characterizations. I am thankful to Biju Boro for SEM measurements. I acknowledge Mrinmoy Gohain for helping me with FESEM characterizations. I am also thankful to Prakash Kurmi and Tridib R. Nath for X-Ray Diffraction; Naba Gogoi for nitrogen adsorption desorption and Fourier-transform infrared spectroscopy characterization at SAIC, Tezpur University. I offer my thanks to Sankur da for helping me with FTIR characterization. I acknowledge all the other technical staff of SAIC, Tezpur University for their cooperation and help. I acknowledge CSIR-NEIST for the FESEM facility.

I am grateful to all the technical staff of department of Physics for their timely support. I offer my gratitude to official staff Patir da and Narayan da for their cooperation and help in all official matters. Their amiable nature makes the official work easier than it seems.

My deepest gratitude to all the past and present members of Material Research Laboratory (MRL), Department of Physics: Rituraj da, Madhabi ba, Bhagyalakhi ba, Devalina ba, Ankush, Kakoli, Atowar, Sushmita and Arnab, for their immense support, suggestions, discussions, motivation and timely help during my PhD tenure. I deeply offer my heartfelt gratitude to them for being generous and loving. I am grateful to get the opportunity to work with them and share a special bond.

I sincerely thank all the past and present members of Advanced Functional Material Laboratory (AFML); Kashmiri ba, Sushant bhaiya, Meenakshi, Mayuri, Korobi, Monika, Saransha, Sayoree, Liyenda, Anil, Deepshekhar, Snehasish and Jafard for their amicable nature, generosity, incredible help and support whenever required. Special thanks to Sushant bhaiya for his motivation and support during the initial days of my PhD.

- -

Special thanks to my friend Sunny for the motivation, support and help during the time I needed it the most. Special acknowledgment goes to my colleagues cum friends: Ashamoni ba, Priyanka ba, Sanghamitra, Jimly, Stuti, Nishant, Sritam, for their help and motivation throughout my PhD journey. I am also thankful to my hostel mates Smita, Juri, Happy, Niharika, Suman, Asfi for their timely help and making my hostel life delightful. Thank you for being such a wonderful friend and making my stay in Tezpur University happier, memorable and worth living.

Now its turn to express my deepest gratitude and appreciation to my parents Mr. Rajani Baruah and Mrs. Bina Baruah for showering me with unconditional love and limitless support and for being empathetic. Their belief in me, encouragement, scarifices and patience have been my driving force to get control of every difficulty that came my way during my PhD journey. Without their blessings and motivation, this journey would have been impossible. These mere words are not enough to express my love and gratitude towards them. I am thankful to my elder sister Kasturee Baruah and my brother-in-law Abhinab Gogoi for their immense love and support. I am grateful to my special friend Ronoj for being there with me always and being my support system during my hard times.

I would like to express my gratitude to everyone whose names could not be mentioned, yet whose assistance have been invaluable to the completion of this thesis.

Last but not the least, I owe all my achievements and accomplishments to the Almighty

for granting me good health, courage, patience and strength to pursue my PhD and move forward in life happily.

xi

Kashmiri Barnah

(Kashmiri Baruah)

Date: 07/11/2024Place: Tezpure

List of Tables

| Table No. | Table caption | Page No. |
|-----------|---|----------|
| Table 1.1 | Classification of Fuel Cells | 3-4 |
| Table 2.1 | Anodic peak potential, peak current density and peak-to- | 48 |
| | peak separation of the electrodes at 20 mV/s scan rate | |
| Table 2.2 | Comparison of the MOR current density of different | 53 |
| | anode catalysts. | |
| Table 3.1 | α and k_s value of the electrodes | 85 |
| Table 3.2 | Tafel slope, Electron transfer coefficient, Calculated | 91 |
| | values of current retention and Deterioration rate of all | |
| | the electrodes | |

List of Figures

| Figure No. | Figure caption | Page No. |
|------------|---|-------------|
| Figure 1.1 | Schematic of the mechanism of DAFC in acidic medium | 2 |
| Figure 1.2 | Schematic of the mechanism of DAFC in basic medium | 2 |
| Figure 1.3 | Schematic of DMFC setup | 8 |
| Figure 1.4 | Schematic of charge storage mechanism in electric double | 17 |
| | layer capacitor | |
| Figure 2.1 | Synthesis route of the nanocomposite Ti_3C_2/Co_3O_4 | 36 |
| Figure 2.2 | FESEM images of (a), (b) Co ₃ O ₄ nanoparticles; (c)-(f) | 38 |
| | Ti_3C_2/Co_3O_4 | |
| Figure 2.3 | (a)-(b) TEM images of $Ti_3C_2NH_4T_x$ nanosheets, (c) Lattice | 39 |
| | fringes (Inset-SAED pattern) of Ti_3C_2 nanosheets, (d)-(e) | |
| | TEM images of Ti_3C_2/Co_3O_4 . (Inset in fig. 2.3e is the lattice | |
| | fringes of Ti ₃ C ₂ nanosheets shown inside circle in fig. 2.3d), | |
| | EDX spectra of (f) Ti_3C_2 , and (g) Ti_3C_2/Co_3O_4 | |
| Figure 2.4 | XRD patterns of (i) Ti ₃ AlC ₂ , (ii) Ti ₃ C ₂ NH ₄ T _x , (iii) DMSO | 40 |
| | intercalated $Ti_3C_2NH_4T_x$, (iv) delaminated $Ti_3C_2NH_4T_x$, and | |
| | (v) Ti ₃ C ₂ /Co ₃ O ₄ . (Symbols signifying: \clubsuit AlF ₃ , \blacklozenge (NH ₄) ₃ AlF ₆ , | |
| | ♥ AlF ₃ .3H ₂ O, $♠$ (NH ₄)AlF ₄ and $●$ TiO ₂) | |
| Figure 2.5 | FTIR of (a) Ti_3AlC_2 and $Ti_3C_2NH_4T_x$, (b)-(c) Ti_3AlC_2 , (d) Co_3O_4 nanoparticles and nanocomposite Ti_3C_2/Co_3O_4 | 43 |
| Figure 2.6 | (a) XPS survey spectra of Co ₃ O ₄ and nanocomposite | 44 |
| | Ti_3C_2/Co_3O_4 ; High resolution XPS spectra of Co 2p in (b) | |
| | Co_3O_4 , and (c) Ti_3C_2/Co_3O_4 ; High resolution spectra of (d) Ti | |
| | 2p, and (e) C 1s of nanocomposite Ti_3C_2/Co_3O_4 | |
| Figure 2.7 | N_2 adsorption-desorption isotherms of (a) $Ti_3C_2,$ (c) Co_3O_4 and | 45 |
| | (c) Ti_3C_2/Co_3O_4 . Inset- Pore size distribution curves of the | |
| | corresponding samples | |
| Figure 2.8 | Electrochemical behaviour of the electrodes in 0.5 M NaOH | 46 |
| | solution (absence of methanol)-Cyclic voltammetry of (a) | |
| | Co_3O_4/GC at 20 mV/s scan rate, (b) Ti_3C_2/GC , Co_3O_4/GC and | |

 $Ti_3C_2/Co_3O_4/GC$ at 20 mV/s scan rate (Inset: Peak-to-peak separation graph at 20 mV/s scan rate), (c) Co_3O_4/GC at (20-200) mV/s scan rate, (d) $Ti_3C_2/Co_3O_4/GC$ at (20-200) mV/s scan rate

- Figure 2.9 (a), (b): I_p vs. v plot of Co₃O₄/GC and Ti₃C₂/Co₃O₄/GC 49 respectively. (c), (d): I_p vs. v^{1/2} plot of Co₃O₄/GC and Ti₃C₂/Co₃O₄/GC respectively
- Figure 2.10 (a) Plot of logarithm of peak anode current density vs. 50 logarithm of scan rate, Laviron's plot: Anodic and cathodic peak potential (v) vs logarithm of scan rate (b) Co₃O₄/GC, (c) Ti₃C₂/Co₃O₄/GC
- Figure 2.11 Electrochemical behaviour of the electrodes in presence of 52 methanol-Cyclic voltammograms of (a) Ti_3C_2/GC , Co₃O₄/GC, Ti₃C₂/Co₃O₄/GC at 20 mV/s in 0.5 M NaOH solution containing 1.5 M methanol, (b) Co₃O₄/GC, and (c) Ti₃C₂/Co₃O₄/GC in 0.5 M NaOH solution containing varying concentration of methanol at 20 mV/s (d) Co₃O₄/GC in 1.5 M methanol solution with varying scan rate from 20-200 mV/s, (e) $Ti_3C_2/Co_3O_4/GC$ electrode in 1.5 M methanol solution with varying scan rate from 20-200 mV/s
- Figure 2.12 Cyclic voltammetry of Co₃O₄/GC in 0.5 M NaOH supporting 54 electrolyte in the presence and absence of 1.5 M methanol at 200 mV/s
- Figure 2.13 (a) Tafel plots of Co₃O₄/GC and Ti₃C₂/Co₃O₄/GC in 1.5 M 55 methanol + 0.5 M NaOH at 20 mV/s, (b) Chronoamperogram of Co₃O₄/GC and Ti₃C₂/Co₃O₄/GC electrodes in 0.5 M NaOH aqueous solution containing 1.5 M methanol at 0.65 V for 3600s, (c) Nyquist plots of the electrodes, (d) cycling stability of Ti₃C₂/Co₃O₄/GC at 20 mV/s in 1.5 M methanol containing 0.5 M NaOH aqueous solution
- Figure 2.14 (a)-(c) FESEM images, (d) XRD pattern, (e) FTIR spectra of 57 Ti₃C₂/Co₃O₄ after 200 CV cycles in 1.5 M methanol solution

containing 0.5 M NaOH aqueous solution

- Figure 2.15 XPS of Ti_3C_2/Co_3O_4 after methanol oxidation: (a) Survey 58 spectra, High-resolution XPS spectra of (b) Co 2p, (c) Ti 2p, and (d) C 1s
- Figure 3.1 Morphology of NCO: (a), (b) FESEM images, (c), (d) TEM 72 images, (e) SAED pattern
- Figure 3.2 Morphology of CNO: (a), (b) FESEM images, (c)-(d) TEM 72 images
- Figure 3.3 Morphology of CNO: (a)-(b) TEM images, (c) SAED pattern 73
- Figure 3.4 Morphology of CNOG: (a), (b)- FESEM images, (c)-(d) TEM 74 images.
- Figure 3.5 Morphology of CNOG: (a)-(c) TEM images. Yellow circle in 75 fig. 3.5b is representing the area magnified in fig. 3.5c
- Figure 3.6 Morphology of CNOG: (a)-(c) TEM images. Red and yellow 76 circles in fig. 3.6a are representing the area magnified in fig.
 3.6b and 3.6c respectively, (d) SAED pattern
- Figure 3.7 EDX spectra of NCO, CNO, and CNOG 76
- Figure 3.8 Elemental Mapping of CNOG: (a) SEM image, (b)-(e) 77 Mapping images of Co, Ni, O, and C respectively, (f) Superimposed image of Co, Ni, O and C
- Figure 3.9 Structural characterizations: (a) XRD pattern of NCO, CNO 78 and CNOG, (b) XRD of GO, (c) FTIR spectra of CNO, GO and CNOG, (d) Raman spectrum of GO
- Figure 3.10 XPS of CNO and CNOG: (a) Survey spectra, High-resolution 80 XPS spectra of (b) Ni 2p, (c) Co 2p, (d) O 1s, and (e) C 1s
- Figure 3.11 N₂ adsorption-desorption isotherms along with pore size 81 distribution in inset (i) NCO, (ii) CNO, (iii) CNOG
- Figure 3.12 Cyclic voltammetry of the electrodes in 0.5 M NaOH (a) 82 NCO/GC, CNO/GC and CNOG/GC at a 10 mVs⁻¹, (b) NCO/GC, (c) CNO/GC, (d) CNOG/GC at varying scan rate
- Figure 3.13 (a), (b), (c): I_p vs. v plot of NCO/GC, CNO/GC, and 83 CNOG/GC respectively, (d), (e), (f): I_p vs. v^{1/2} plot of

NCO/GC, CNO/GC, and CNOG/GC respectively

- Figure 3.14 (a) Plot of logarithm of peak anode current density vs. 84 logarithm of scan rate, Laviron's plot: (b) NCO/GC, (c) CNO/GC, (d) CNOG/GC
- Figure 3.15 Cyclic voltammetry in presence of methanol: (a) NCO/GC, 86 CNO/GC, and CNOG/GC at 50 mVs⁻¹ in 0.5 molar sodium hydroxide solution in 3 molar CH₃OH, (b) NCO/GC, (c) CNO/GC, (d) CNOG/GC at varying concentrations of CH₃OH at 200 mV/s
- Figure 3.16 Cyclic voltammetry in presence of methanol: (a) NCO/GC, 87
 (b) CNO/GC, and (c) CNOG/GC in 3 molar CH₃OH at varying scan rate
- Figure 3.17 Tafel plot in 3 M methanol at 10 mVs⁻¹: (a) NCO/GC, (b) 88 CNO/GC at low overpotential, (b) CNO/GC at high overpotential, (d) CNOG/GC at low over potential, (b) CNOG/GC at high over potential
- Figure 3.18 (a) Chronoamperograms of NCO/GC, CNO/GC, and 89 CNOG/GC in 3 molar CH₃OH at 0.65 V for 1 hr, (b) Nyquist plots (Top inset: zoomed view of higher frequency Nyquist plot, bottom inset: equivalent circuit), (c) Cycling stability of CNOG/GC at a 30 mVs⁻¹ in 3 molar CH₃OH
- Figure 3.19 XPS of CNOG after methanol oxidation: (a) Survey spectra, 92 High-resolution XPS spectra of (b) Ni 2p, (c) Co 2p, (d) O 1s, and (e) C 1s
- Figure 3.20 Characterizations of CNOG after methanol oxidation: (a)–(c) 93
 FESEM images. In fig. 3.20a, the red circles are displaying the lumps and blue circles marking the fragmentation of NiCo₂O₄ flakes, (d) XRD, and (e)-(f) FTIR pattern after 1000 CV cycles in 3 molar CH₃OH + 0.5 molar sodium hydroxide aqueous solution
- Figure 3.21 FESEM of CNOG after methanol oxidation: (a) Enlarged 94 image of fig. 3.20a. Red circles are marking the lumps, (b) Enlarged image of fig. 3.20a. The areas marked by blue

circles are displaying the non-uniform restacking and fragmentation of $NiCo_2O_4$ flakes, (c) Magnified image of the lumps shown inside red circle in fig. 3.21a

- Figure 4.1 Morphological characterizations of CNOT: (a)-(b) FESEM 106 images, (c)-(d) TEM images
- Figure 4.2 Morphological characterizations of CNOT: (a) HRTEM 106 image with d-value, (b) SAED pattern, (c) Particle size distribution of CNO in CNOT
- Figure 4.3 Morphology of NCO: (a) SAED pattern, (b)-(c) HRTEM 107 images, (d) Grain size distribution of NCO
- Figure 4.4 EDX spectra: (a) Etched MXene, (b) CNOT 108
- Figure 4.5 (a) XRD of (i) MXene, (ii) delaminated MXene, (iii) CNOT, 109(b) FTIR of CNOT
- Figure 4.6 N₂ adsorption-desorption isotherms of CNOT. Inset-Pore size 110 distribution curve
- Figure 4.7 (a) Cyclic voltammetry of CNOT/GC in 0.5 molar sodium 111 hydroxide, Plot of (b) I_p vs. v, (c) I_p vs. v^{1/2}, (d) log I_p vs log v,
 (e) Laviron's plot: Anodic and cathodic peak potential (V) vs logarithm of scan rate of CNOT
- Figure 4.8 Cyclic voltammetry in presence of methanol: (a) different 113 concentration of methanol at 10 mV/s, (b) 5 M methanol concentration, Tafel plots of CNOT/GC in 5 M methanol at 10 mVs^{-1} , (c) low overpotential, (d) high overpotential
- Figure 4.9 (a) Chronoamperometry in 5 M methanol at 0.65 V for 1 hr, 114
 (b) Nyquist plot of CNOT in 5 M methanol solution. (Left inset: zoomed image of high frequency region Nyquist plot, Right inset: Equivalent circuit), (c) Cycling stability at 20 mVs⁻¹ in 5 M methanol. The supporting electrolyte is 0.5 M NaOH aqueous solution
- Figure 4.10 (a) XPS spectra of CNOT before and after methanol 117 oxidation: (a) Survey spectra; High-resolution spectra of (b) Ni 2p, (c) Co 2p, (d) Ti 2p, (e) C 1s, and (f) O 1s
- Figure 4.11 Post methanol oxidation characterizations of CNOT: (a)–(c) 118

FESEM micrographs, (d) XRD pattern, and (e) FTIR spectra

- Figure 5.1 (a) Cyclic voltammetry in 3M KOH at 10 mV/s scan rate, 127 Cyclic voltammetry of CNOG at (b) higher scan rate, (c) lower scan rate
- Figure 5.2 Galvanostatic charge-discharge (GCD) measurements of (a) 128
 NCO, CNO and CNOG at 1 A/g current density; (b) NCO, (c)
 CNO, and (d) CNOG from 0.5 to 10 A/g, (e) Nyquist plot of the electrodes (inset: equivalent circuit), (f) Cycling stability of CNOG and CNO at 10 A/g current density
- Figure 5.3 Post cycling stability test of CNOG: (a), (b) FESEM images 131 at different magnifications, (c) EIS (Inset: Equivalent circuit)
- Figure 5.4 Electrochemical study of symmetric supercapacitor 132 CNOG//CNOG in 3M KOH aqueous electrolyte: (a) Cyclic voltammogram of different potential windows, (b) Comparing windows 0.85 V, 0.90 V and bare graphite at 50 mV/s, (c) Cyclic voltammogram in (0 to 0.9) V window at varying scan rate, (d) Nyquist plot. (Top inset: magnified view of higher frequency Nyquist plot, bottom inset: equivalent circuit)
- Figure 5.5 Electrochemical study of symmetric supercapacitor 133 CNOG//CNOG in 3M KOH aqueous electrolyte: (a) GCD at varying current densities, (b) Specific capacitance vs. current density plot, (c) Specific capacitance up to 4500 GCD cycles (Inset: First two and last two cycles)
- Figure 5.6 Structural and morphological characterizations after cycling 135 stability of the symmetric supercapacitor electrode: (a) XRD pattern of CNOG, (b) XRD of bare graphite, (c) Magnified view of XRD peaks of active material; with symbols signifying: ★ Co₂O₄ ★ NiO ♥ Ni(OH)₂ ♦ NiCo₂O₄ phase), (d)-(f) FESEM images
- Figure 5.7 Two-electrode electrochemical characterization of symmetric 137 supercapacitor CNOG//CNOG in hydrogel polymer electrolyte PVA/3M KOH: (a) Cyclic voltammetry in different potential window, (b) Cyclic voltammograms in (0

xxiii

to 1.3) V with varying scan rate, (c) Galvanostatic chargedischarge curves at varying current density, (d) Specific capacitance vs. current density plot, (e) Ragone plot, (f) Specific capacitance with cycle number (Inset: First two and last two cycles)

- Figure 5.8 (a) 2 CNOG//CNOG cells in series, (b) 1.8 V LED glow with 138 4 cells in series
- Figure 6.1 3-electrode electrochemical characterizations in 3M KOH: 149
 Cyclic voltammetry of (a) All electrodes at 10 mV/s scan rate,
 (b) MXene, (c) CNOT at high scan rate, (d) CNOT at low scan rate
- Figure 6.2 3-electrode electrochemical characterizations in 3M KOH: 151
 Galvanostatic charge-discharge of (a) All electrodes at 1 A/g
 current density, (b) MXene from 0.5 to 10 A/g, (c) CNOT
 from 0.5 to 10 A/g current density, (d) Nyquist plot (Left
 inset: magnified view of higher frequency region of Nyquist
 plot, Right inset: Equivalent circuit), (e) Cycling stability of
 CNOT at 10 A/g
- Figure 6.3 Post cycling stability test of CNOT: (a) EIS (Inset: Equivalent 153 circuit), (b)-(c) FESEM images
- Figure 6.4 Two-electrode electrochemical characterization of symmetric 154 supercapacitor CNOT//CNOT in 3M KOH: (a) Cyclic voltammetry in different potential window, (b) GCD at 0.5 A/g for different potential windows, (c) CV of CNOT//CNOT and bare graphite//bare graphite at 50 mV/s in window (0 to 0.9) V
- Figure 6.5 Two-electrode electrochemical characterization of symmetric 155 supercapacitor CNOT//CNOT in 3M KOH: (a) Cyclic voltammograms in (0 to 0.9) V with varying scan rate, (b) Galvanostatic charge-discharge at varying current density, (c) Specific capacitance vs. current density plot, (d) Specific capacitance with cycle number (Inset: Two cycles from first and last), (e) Nyquist plots (Left inset: magnified view of the

higher frequency region Nyquist plot, Right inset: Equivalent circuit)

- Figure 6.6 Two-electrode electrochemical characterization of symmetric 157 supercapacitor CNOT//CNOT in hydrogel polymer electrolyte PVA/3M KOH: (a) Cyclic voltammetry in different potential window, (b) Cyclic voltammograms in (0 to 1.4) V with varying scan rate, (c) Galvanostatic chargedischarge curves at varying current density, (d) Specific capacitance vs. current density plot, (e) Specific capacitance with cycle number (Inset: First two and last three cycles), (f) Ragone plot
- Figure 6.7 Structural and morphological characterization of CNOT after 159
 4500 GCD cycles of the symmetric supercapacitor
 CNOT//CNOT: (a) XRD pattern of CNOT, (b) Magnified
 view of XRD peaks of active material; with symbols
 signifying: ♠ Co₂O₄ ♠ NiO ♥ Ni(OH)₂ ♠ NiCo₂O₄ phase and
 MXene, (c) XRD of bare graphite, and (d)-(f) FESEM
 images
- Figure 6.8 Four CNOT//CNOT cells in series, (b) Charging of 4 cells, 160 (c)-(d) 1.8 V LED glow with 4 cells in series

List of Abbreviations

| Abbreviations | Meaning |
|---------------|--|
| FC | Fuel Cell |
| DAFC | Direct Alcohol Fuel Cell |
| HOR | Hydrogen Oxidation Reaction |
| ORR | Oxygen Reduction Reaction |
| AFC | Alkaline Fuel Cell |
| PEMFC | Proton exchange membrane fuel cell |
| SPFC | Solid Polymer Fuel Cell |
| SPEFC | Solid Polymer electrolyte Fuel Cell |
| PEFC | Polymer Electrolyte Fuel Cell |
| PEMFC | Polymer Electrolyte Membrane Fuel Cell |
| PAFC | Phosphoric Acid Fuel Cell |
| MCFC | Molten Carbon Fuel Cell |
| SOFC | Solid Oxide Fuel Cell |
| DMFC | Direct Methanol Fuel Cell |
| DEFC | Direct Ethanol Fuel Cell |
| AAEMFC | Alkaline Anion Exchange Membrane Fuel Cell |
| AEM | Anion-exchange Membrane |
| ADMFC | Alkaline Direct Methanol Fuel Cell |
| MOR | Methanol oxidation reaction |
| MEA | Membrane Electrode Assembly |
| GDL | Gas Diffusion Layers |
| PSSA | Polystyrene Sulfonic Acid Membrane |
| PFSA | Perfluorosulfonic Acid |
| PGMs | Pt-group metals |
| CL | Catalyst Layer |
| MPL | Microporous Layer |
| PTFE | Polytetrafluoroethylene |
| TPB | Triple Phase Boundary |
| | |

| EDLC | Electric double layer capacitors |
|-----------------|---|
| ТМО | Transition Metal Oxide |
| FESEM | Field Emission Scanning Electron Microscopy |
| TEM | Transmission Electron Microscopy |
| XRD | X-ray Diffraction |
| FTIR | Fourier-Transform Infrared Spectroscopy |
| XPS | X-ray Photoelectron Spectroscopy |
| BET | Brunauer-Emmett-Teller |
| BJH | Barret-Joyner-Halenda |
| EDX | Energy Dispersive X-ray |
| CV | Cyclic Voltammetry |
| CA | Chronoamperometry |
| EIS | Electrochemical impedance spectroscopy |
| GCD | Galvanostatic charge-discharge |
| NRP | Nanorod Pellet |
| DMSO | Dimethyl Sulfoxide |
| GCE | Glassy Carbon Electrode |
| MX | MXene |
| NW | Nanoworm |
| PDDA | Poly-(diallyldimethyl-ammonium chloride) |
| RHE | Reversible Hydrogen Electrode |
| CNT | Carbon Nanotube |
| NP | Nanoparticle |
| PANI | Polyaniline |
| SAED | Selected Area Electron Diffraction |
| SWCNT | Single Walled Carbon Nanotube |
| PVA | Polyvinyl alcohol |
| CPE | Constant phase element |
| CO ₂ | Carbon dioxide |
| H_2 | Hydrogen |
| O ₂ | Oxygen |
| N ₂ | Nitrogen |
| СО | Carbon monoxide |
| | |

| CH₃OH | Methanol |
|----------------------------------|---------------------------------|
| H ₂ O | Water |
| H^{+} | Hydrogen ion |
| OH- | Hydroxyl ion |
| MnCo ₂ O ₄ | Manganese Cobaltide |
| CoCo ₂ O ₄ | Cobalt Oxide |
| NiCo ₂ O ₄ | Nickel Cobaltite |
| NiO | Nickel oxide |
| rGO | Reduced Graphene Oxide |
| С | Carbon |
| 0 | Oxygen |
| HF | Hydrofluoric Acid |
| LiF | Lithium Fluoride |
| HCl | Hydrochloric Acid |
| NH ₄ HF ₂ | Ammonium Bifluoride |
| F | Fluoride ion |
| O ²⁻ | Oxide ion |
| CoO | Cobalt (II) Oxide |
| Co_2O_3 | Cobalt (III) Oxide |
| CoO_2 | Cobalt (IV) Oxide |
| Co_3O_4 | Cobalt (II, III) Oxide |
| Ti ₃ AlC ₂ | Titanium Aluminium Chloride |
| $Co(NO_3)_2 \cdot 6H_2O$ | Cobalt (II) Nitrate Hexahydrate |
| NaOH | Sodium Hydroxide |
| Ag | Silver |
| AgCl | Silver Chloride |
| Ti | Titanium |
| С | Carbon |
| 0 | Oxygen |
| Со | Cobalt |
| Al | Aluminium |
| Ν | Nitrogen |
| F | Fluorine |

| Pt | Platinum |
|--|-------------------------------|
| Pd | Palladium |
| СоООН | Cobalt oxyhydroxide |
| NiOOH | Nickel oxyhydroxide |
| КОН | Potassium Hydroxide |
| Co(OH) ₂ | Cobalt (II) hydroxide |
| Co(NO ₃) ₂ .6H ₂ O | Cobaltous Nitrate Hexahydrate |
| GO | Graphene Oxide |
| Ni | Nickel |
| MoS_2 | Molybdenum disulfide |
| AlF ₃ | Aluminium Fluoride |
| $(NH_4)_3AlF_6$ | Ammonium hexafluoroaluminate |
| RuO ₂ | Ruthenium (IV) Oxide |
| ZnO | Zinc Oxide |
| MnO ₂ | Manganese dioxide |

List of Symbols

| Symbols | Meaning |
|-----------------|-------------------------------|
| E _p | Peak potential |
| E _{pa} | Anodic peak potential |
| E _{pc} | Cathodic peak potential |
| ΔE_p | Peak to peak separation |
| Ip | Peak current |
| I _{pa} | Anodic peak current |
| I _{pc} | Cathodic peak current |
| ν | Scan rate |
| Eo | Formal potential |
| Io | Exchange current density |
| F | Faraday constant |
| Γ^* | Surface coverage |
| Z' | Real impedance |
| Ζ'' | Imaginary impedance |
| А | Geometric surface area |
| R | Gas constant |
| Т | Absolute temperature |
| α | Electron transfer coefficient |
| ks | Heterogeneous rate constant |
| Ω | Ohm |
| h | hour |
| A/g | Ampere per gram |
| C_{sp} | Specific Capacitance |
| F/g | Farad per gram |
| E | Energy density |
| Р | Power density |
| Wh | Watt-hour |
| Wh/kg | Watt-hour per kilogram |

| Ι | Discharge current |
|-----------------|----------------------------|
| ΔV | Potential window |
| Δt | Discharge time |
| R _s | Series resistance |
| R _{ct} | Charge transfer resistance |
| C _p | Faradaic capacitance |
| W | Warburg impedance |
| S | Siemens |